NIPPON STEEL TECHNICAL REPORT No. 69 APRIL 1996

UDC532.5.011:681.3

# Development of Quantitative Full-Field Velocity Measurement System

Norihisa Tsuda*1 Tsutomu Haeno*1
Tetsuo Saga*2 Toshio Kobayashi*2

**Abstract:**

*Flow-field analysis methods occupy an important position in a variety of industrial fields. Among these, particle imaging velocimetry (PIV) is highlighted as a technique for understanding the spatial structure of complex flow fields and simultaneously measuring the velocity of many points in such flow fields. PIV is making rapid progress as a new tool for measuring flow fields. Nippon Steel has developed and applied a general-purpose PIV system to important development project, as a basic technology for experimentally elucidating fluid dynamic problems in ironmaking and steelmaking processes. Outlined here is the quantitative full-field velocity measurement system designated Current, which was jointly developed by Nippon Steel and the University of Tokyo's Institute of Industrial Science. Examples of its application to water flow, air flow, and two-phase flow of gas and liquid are also described.*

## 1. Introduction

Elucidation of flow-field phenomena occupies an important position in a variety of engineering fields. Techniques for measuring velocity using laser and hot-wire velocimeters have long been studied, resulting in a substantial amount of data. More recently, powerful computers have become commonly available and extensively used to investigate flow-field prediction techniques. The computer-based prediction of flow fields is expected to have practical applications in the near future.

The quantitative full-field velocity measurement system reported here is a new fluid measuring method that digitally processes visualized images of a flow field and from these images determines flow field velocities. It is highlighted as an effective tool for instantaneously collecting velocity information at many two-dimensional and three-dimensional points[1-4]. Known as a particle imaging velocimeter, this system is being applied in many areas, including the development of plants, automobiles, ships, aircraft and buildings, and in the basic and applied research of flow-field control for semiconductors and biotechnology. The greatest challenges facing the developers of the quantitative full-field velocity measurement system designated Current are promptly processing experimental results and adapting it to various flow fields. Developed to meet these needs, the Current is enabling a variety of studies to be more efficiently carried out than in the past.

## 2. Imaging Velocimeter

Imaging velocimeters can be classified into three categories: particle tacking velocimetry (PTV) whereby tracer particles are added into a flow field and tracked at given time intervals to compute their velocities in the flow field; particle imaging velocimetry (PIV) whereby the flow velocity of tracer particles is calculated from the similarity between the distribution patterns of tracer particles at different times; and laser speckle velocimetry (LSV) whereby the speckle pattern of scattered particles in a flow field

*1 Kimitsu Works

*2 The University of Tokyo

is recorded as a double-exposure photograph and the movement distance of the speckle pattern is measured from the speckle photograph. The first characteristic of these measuring systems is the simultaneous measurement of many points in the flow field. This is extremely helpful in measuring a three-dimensional flow with a complex channel shape, as handled in the area of engineering. The second characteristic is the simultaneous measurement of two or three velocity components. In the development and verification of turbulent flow models, information about the Reynolds stress tensor and higher-order turbulent flow statistics is useful. There is an extremely high demand for the simultaneous measurement of multiple velocity components.

PTV and PIV are trouble-free flow visualization techniques suited for practical use in model experiments conducted to gain an understanding of plant phenomena in the ironmaking and steelmaking processes. Nippon Steel's Kimitsu Works developed Current PTV and Current PIV as velocimetric techniques for liquid and air flows, respectively. They are used in various model experiments. The following chapters outline the PTV system that has been already developed and the PIV system that is under development, and include the results of velocity measurements conducted in flow fields.

## 3. Development of PTV and PIV System

The quantitative full-field velocity measurement system, Current, consists of optical and image processing systems. The optical system is composed of a laser light sheet (LLS) and a TV camera of the NTSC (National Television System Committee) type. The image processing system is based on a personal computer. The development of the Current took particular account of the following points:

(1) Existing PTV systems are effective for flows of a relatively low Reynolds number, but find it often difficult to handle flows of a high Reynolds number. This is because TV cameras and recorders of the NTSC type, which have excellent performance and versatility, are used as image input devices. Their speed of 30 frames per second makes it impossible to track tracer particles when the tracer particles rapidly move in the space to be visualized. Current intermittently emits a laser light sheet (LLS) into the fluid in question and follows tracer particles from each frame of the image obtained. This design has enabled it to measure flow fields with high Reynolds numbers.

(2) To maintain measurement accuracy, PTV requires the selection of tracer particles of approximately the same density as that of the fluid concerned and of small size. As long as NTSC-type TV cameras and recorders are used, however, the positions of tracer particles cannot be detected if the tracer particle images are equal to or lower in resolution than the TV camera's CCD. With Current, tracer particle images of lower spatial resolution than that of the TV camera are formed on each image frame, and the tracer particle positions can be accurately detected from the resultant weak images by a newly developed image improvement algorithm.

(3) The velocity in air flow visualization experiments can be determined by the cross-correlation technique from two tracer particle images 1 $\mu$m or smaller obtained as experimental results.

(4) An algorithm for interpolation on grid points and high-seed computing algorithms for the Poisson and Laplace equations, among other things, have been developed so that the PTV and the PIV systems can measure time-averaged velocity, turbulence intensity, and Reynolds stress and pressure from momentary velocities in the flow field to be visualized.

(5) A low-cost image processing system was built based on a personal computer. After considering the speeding up of processing and development flexibility, software described in the C language and the ASM language was adopted for the image processing system. The developed software is about 10 MB in an execution module or EXE format.

## 4. Configuration of PTV and PIV System

PTV and PIV two-dimensionally track the motion of tracer particles added into a flow and measure two velocity components at short time intervals. To analyze the motion of tracer particles moving from low to high velocities, a visualization system and an image processing systems have been constructed as described below.

### 4.1 Configuration of visualization system

**Fig. 1** shows the visualization system that consists of an optical system, image processing, input and recording devices, and their controller. A 4-W argon laser is used as the light source. The laser beam passes the acousto-optic cell (AOM), where it is scattered due to the Doppler effect. The primary scattered laser light is introduced into the optical fiber. That is, the AOM is tuned on and off to intermittently illuminate a flow field with pulses within a short period of time. The laser light leaving the end of the optical fiber is formed into a laser light sheet (LLS) of a few millimeters thickness by two cylindrical lenses and multiple optical lenses. The AOM and the TV camera are controlled by an external controller to set the illumination timing of the LLS with respect to the vertical and horizontal synchronization of the TV camera.

**Fig. 2** shows an example of LLS illumination timing. The LLS is momentarily emitted once in the first half of the first field and thrice in the last half of the second field. The LLS illumination time Ti and interval di can be controlled in 1-$\mu$s increments according to flow velocity. The LLS illumination frequency can be selected as required.

To process visualization images by the PTV technique, the frame accumulation method shown in **Fig. 2** is adopted for the TV camera. That is, the laser light is directed onto the CCD device of the first field for 1/30 of a second from the start of the first field to the end of the second field and onto the CCD device of the second field for 1/30 of a second from the start of the second field to the end of the first field of the next frame. When the above-mentioned illumination code is used, therefore, the tracer

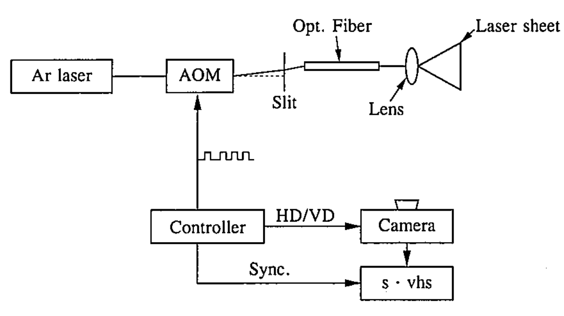


**Fig. 1** Visualization optical system

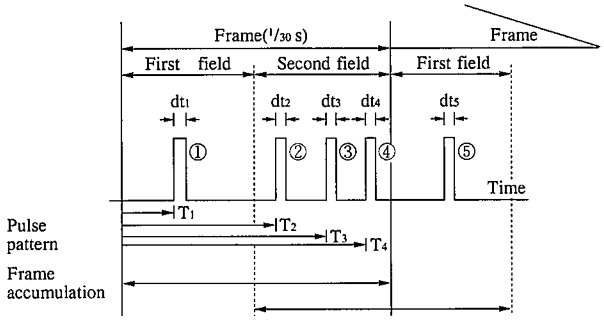


Fig. 2 LLS illumination code

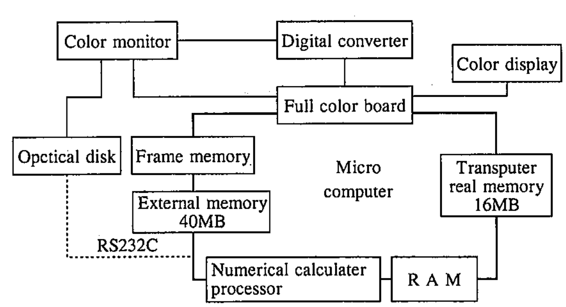


Fig. 3 Image processing system

particle images photographed as illuminated with the LLS at the times T1 and T5 are recorded only in the photosensors of the first field. The tracer particle images photographed as illuminated with the LLS at the times T2 to T4 are recorded in the photosensors of both fields due to the frame integration time overlap. In PTV processing, the representative position of the tracer particles is defined as the center of gravity of the particle image. The velocity calculation thus uses the center of gravity of the particle images recorded at the times T2 to T4 when the center of gravity position is accurately measured.

The visualization images are processed by the PIV technique as follows. When the tracer particles move over a short distance in the visualization space, the field integration method is adopted by the TV camera. The second field is illuminated once with the LLS, and the velocity is measured from images recorded twice per frame by tracking the tracer particles. When the tracer particles move over a longer distance in the visualization space, the field integration method is adopted for light accumulation. That is, the light from the flow field is directed onto the CCD device of the first field for 1/60 of a second from the start to the end of the first field and onto CCD device of the second field for 1/60 of a second from the start to the end of the second field. The LLS illumination is made once each in the first and second fields. The velocity is measured from the continuous per-field images by tracking the tracer particles.

The LLS illuminations based on the LLS illumination code are performed in continuous TV frames. The TV camera output signals are transmitted and recorded as NTSC standard composite signals.

### 4.2 Image processing system

The video signals obtained in this way are selectively recorded on an optical disk. The video signals recorded on the optical disk are then input frame by frame into the frame board of the image processing system shown in **Fig. 3**, and converted into digital images with 512 × 480 pixels and 8 bits. In addition, the TV camera output signals can be directly input into the frame memory of the image processing system. Based on the 32-bit microcomputer, the image processing system consists of the frame board that complies with the NTSC standard, a full-color board that displays the calculated results, and an external magnetic disk drive unit that stores the calculated results.

The main processing operations performed by the image processing system are: (1) input of visualization images, improvement of images, elimination of noise, and measurement of center of gravity of tracer particles (for PTV); (2) tracking of tracer particles, calculation of velocity vectors, interpolation to arbitrary wire frame, and conversion to various physical quantities; and (3) representation of processing results by computer graphics.

## 5. Image Processing and Velocity Measurement in PTV

The tracer particle images obtained by the above-mentioned visualization system are preprocessed to improve quality and remove noise. Using the images, the velocity vectors are measured next by the motion analysis of the tracer particles. The PTV system determines two-dimensional velocity vectors based on the information about each frame of input image exposed many times by the coded LLS. The velocity vectors on the grid points are predicted from the measured velocity vectors and converted into various physical quantities, and those results are graphically displayed.

### 5.1 Preprocessing of images

**Fig. 4** shows the density values of white tracer particles (Nylon 12) on input images obtained when the tracer particles were added into a flow channel. The horizontal axis indicates the LLS illumination time interval dt (H), where 1 H is 63.56 $\mu$s. The vertical axis indicates the density of the tracer particles on each input image. The experimental conditions for this visualization were set as follows. The output of the laser was set at 2 W, and the thickness of the LLS was set to 2 mm. The TV camera was vertically set at a distance of about 1 m from the observation plane. The observation plane measured 100 mm × 100 mm in area. From **Fig. 4**, it is evident that the density of the tracer particles on the input image decreases with lower tracer particle diameter and LLS illumination time interval. To measure the velocity of a few meters per second under the above conditions, for example, the LLS illumination time must be set at a few Hs to obtain momentary images. Given their tendecy to bunch-up in fluid, tracer particles measuring 50 $\mu$m or less in diameter must

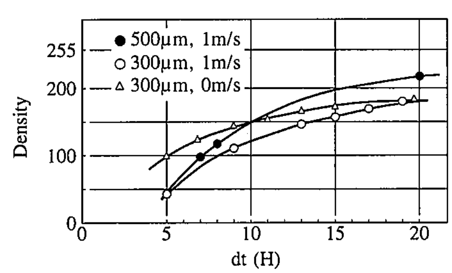


Fig. 4 Relationship between tracer particle diameter and image density

also be selected. The density of the tracer particles obtained on the image under these conditions becomes considerably low and approaches that of the background image. It is thus difficult to isolate such tracer particle images from the background by simple background processing and binarization, and the tracer particles visualized are limited in number.

The following algorithm was developed to improve the tracer particle images. The image improvement algorithm is effective: (1) when the density of individual tracer particles is not markedly different from that of the background image; and (2) when the background image varies in density in spatial and temporal terms and when the thresholding level spatially varies. First, visualization images are introduced into the frame board as frame images every 1/30 of a second. During the A/D conversion of the input image, the voluntary input voltage range of 0 to 1 V of the composite video signals is converted into the digital range of 0 to 255 intensity levels. The image is processed to improve its quality as described below.

First, the input image is averaged by Eq. (1), using the 3 × 3 mask shown in **Fig. 5**.

$$g_0=(f_0+f_1+f_2+f_3+f_4+f_5+f_6+f_7+f_x)/9 \qquad \cdots\cdots(1)$$

where $g_0$ is the density at the center of the averaged output image. Second, the averaged image is Laplacian filtered by Eq. (2).

$$g_0=(f_1+f_3+f_5+f_7)-4f_0 \qquad \cdots\cdots(2)$$

Third, the filtered image is processed to leave only the negative density region, and the negative density region of the filtered image is subtracted from the averaged image. To emphasize the density of the image with respect to the tracer particles, these processing operations are repeated several times according to the density of the input image.

**Fig. 6** shows an example of image improvement. **Fig. 6**(a) shows part of the input image and the density distribution on a line in the image. **Fig. 6**(b) shows the improved image. High-density positions correspond to tracer particles. As can be seen from **Fig. 6**, the image improvement method effectively functions for such images where the density difference between the tracer particles and the background is small and where the background spatially varies in density.

**5.2 Preparation of processing image**

Image analysis prepares a processing image from an input image in the same frame. The image to be used differs with the tracer tracking algorithm employed. Described here is the preparation of processing images as required to measure the velocity of minute tracer particles moving rapidly in a fluid. Two field

| | | |
|---|---|---|
| $f_4$ | $f_3$ | $f_2$ |
| $f_5$ | $f_0$ | $f_1$ |
| $f_6$ | $f_7$ | $f_8$ |

**Fig. 5** 3 × 3 mask

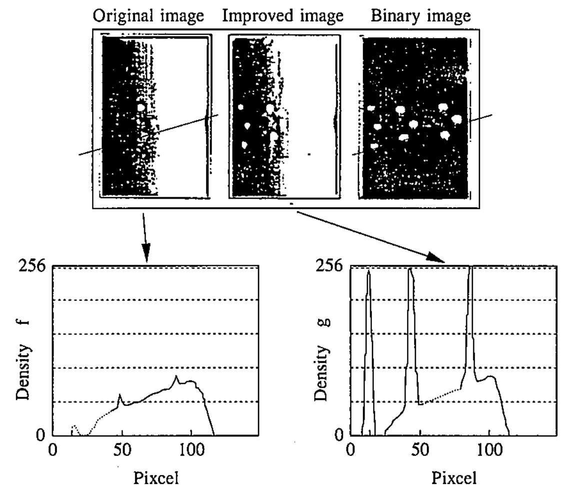


(a) Input image (b) Improved image

**Fig. 6** Tracer particle image and improved image

images are prepared from a single frame image, and velocity vectors are determined from the frame image and the field images. In field image preparation, the field is separated into the first and second fields by using a field separation mask. The density values of image field pixels left blank by this separation are obtained by the interpolation operation of Eq. (3), using the mask of **Fig. 5**.

$$f_0=(f_2+f_3+f_4+f_6+f_7+f_8)/6 \qquad \cdots\cdots(3)$$

The three images are binarized to separate and extract the tracer particles from the background image. The center of gravity of the individual tracer particles is measured from this image and stored in the external memory of the image processor.

**5.3 Determination of velocity vectors**

Described below is the algorithm for analyzing the motion of tracer particles within a short time and for measuring their velocity by using the processing images prepared by the above-mentioned procedure as well as the center-of-gravity information of the tracer particles. This section explains only the algorithm for tracking relatively large tracer particles (about 100 μm in diameter) moving at high velocity. The method of tracking finer tracer particles and other details are reported in Reference [5].

**Fig. 7** shows the basic algorithm to calculate the velocity vectors. The coded LLS illumination and the frame integration of the TV camera produce the tracer particle images ① to ⑤ on the frame image G, the tracer particle images ① to ④ on the first field image G1, and the tracer particle images ② to ⑤ on the second field image G2. ① to ⑤ refer to the tracer particle images photographed as illuminated by the LLS at the times T1 to T5, respectively. The tracer particles are tracked and determined on the frame image G. The frame image G has no time information. The time information of the first and second field images G1 and G2 is used. That is, the first and second field images G1 and G2 are subtracted from each other to eliminate the common particles ② to ④ and extract the particles ① and ⑤. At this time, the particle ① that has a positive density value is the one that existed in the frame image G1 and is thus judged as the start-point particle. Based on this information, the tracer particles are tracked on the frame image G to measure their velocity.

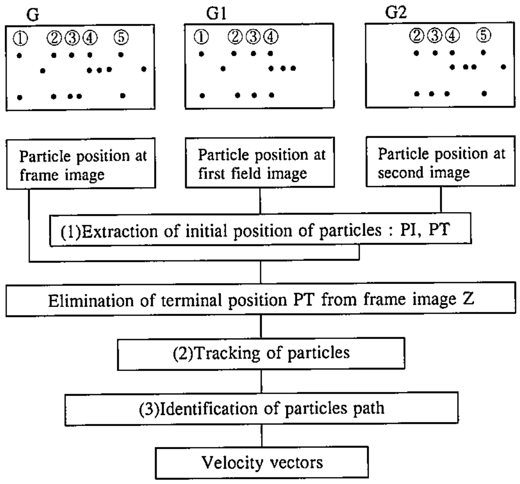


**Fig. 7** Procedure for determining velocity vectors

### 5.4 Prediction of grid point velocity

The velocity vectors obtained by the above-mentioned processing procedure are scattered at arbitrary points in the measurement domain. For this reason, wire frames of equal intervals and non-equal intervals were formed in a flow field, and velocity vectors at grid points were predicted. An interpolation region was established around a grid point as shown in **Fig. 8**, and the velocity vector at the grid point was obtained by interpolation from the velocity vectors present there as described below. The interpolation region is a rectangular region with each side measuring a half of the distance between the adjacent grid points. From the n velocity vectors present in the interpolation region, three arbitrary velocity vector combinations were selected and calculated by the following matrix equation:

$$Ui = U + \frac{du}{dx}dx + \frac{du}{dy}dy$$

$$\begin{bmatrix} 1\,dx_k\,dy_k \\ 1\,dx_l\,dy_l \\ 1\,dx_m\,dy_m \end{bmatrix} \cdot \begin{bmatrix} U \\ \frac{du}{dx} \\ \frac{du}{dy} \end{bmatrix} = \begin{bmatrix} U_k \\ U_l \\ U_m \end{bmatrix} \quad \cdots\cdots(4)$$

where $U_k$, $U_l$ and $U_m$ are three arbitrary combinations of velocity vectors in the interpolation region, and U, du/dx, and du/dy are the velocity vector and velocity vector differential values of the grid point to be interpolated. Similar computation is performed for the $nC_3$ combinations of velocity vectors in the interpolation region. The $nC_3$ interpolation results were averaged to obtain the velocity vector at the grid point in question.

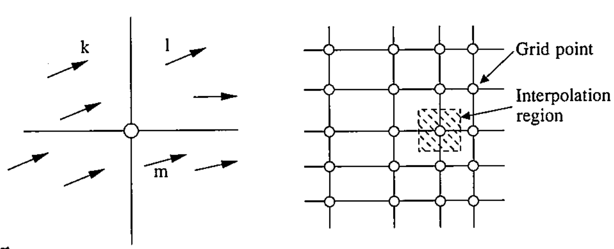


(a) Velocity vectors around grid point

(b) Interpolation region

**Fig. 8** Prediction of velocity vectors around grid point

## 6. Application Example of PTV System

The practicality of the PTV system is presented first. **Fig. 9** is a visualization photograph in a water model experimental apparatus. The experimental apparatus is a 1/7th scale water model of a continuous caster mold used in the continuous casting process. Nylon 12 was used for flow visualization. The experimental apparatus measured 34 mm wide by 212 mm in cross section. A circular submerged nozzle (10 mm ID and 20 mm OD) was inserted to a depth of 30 mm. Near the end of the submerged nozzle were two 10-mm diameter discharge outlets, opened at an angle of 15° to the vertical direction of the submerged nozzle. The flow fully developed in the 1-m long round tube attached to the top of the submerged nozzle and passed through the submerged nozzle into the experimental apparatus. The time average velocity in the submerged nozzle was 1 m/s, and the maximum velocity at the outlets of the submerged nozzle was 1.75 m/s. The flow leaving the submerged nozzle impinged on the sides of the experimental apparatus and separated into upward and downward streams along the wall. Some of the flow formed a cavity at the top of each side, and the rest moved in the direction of gravity toward the bottom of the experimental apparatus.

**Table 1** shows the LLS illumination codes. The LLS was adjusted to a thickness of 1 mm. Since a low-velocity region and a high-velocity region were mixed in the 100 mm × 100 mm measurement domain near the end of the submerged nozzle, input images were prepared by using three levels of LLS illumination codes as shown in **Table 1**.

**Fig. 10** shows the tracer particles tracked from an input image. The tracer tracking results obtained with the LLS illumination codes of **Table 1** are superimposed on the visualization space by linearly setting the time standard at 7 ms. About 600 tracer particle tracking results were obtained by photographing 60 field images. In **Fig. 11**, the velocity vectors calculated by the above-mentioned interpolation method are shown on a 31 × 31 grid. It takes about one minute to make the interpolation calculation after obtaining the flow visualization, demonstrating the practicality of the PTV system.

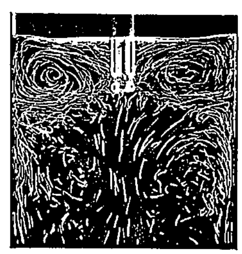

**Fig. 9** Image visualized by tracer particles

**Table 1** LLS illumination codes

| Code | T1 | T2 | T3 | T4 | dt |
|---|---|---|---|---|---|
| 1 | 220H | 270H | 300H | 330H | 10H |
| 2 | 100H | 200H | 400H | 510H | 10H |
| 3 | 100H | ——— | 356H | ——— | 10H |

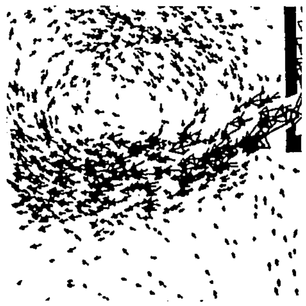

Fig. 10 Tracer tracking results

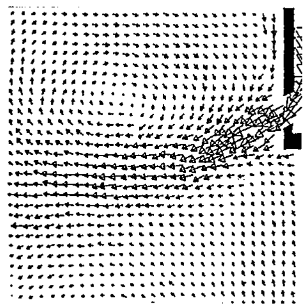

Fig. 11 Velocity vectors on grid points

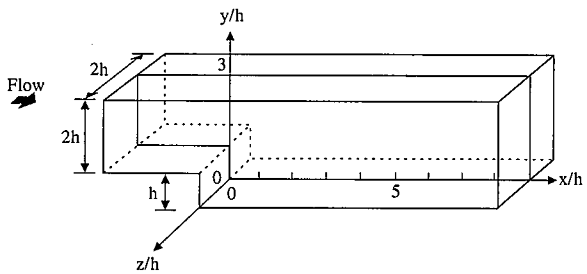


Fig. 12 Measurement of velocity in channel with rearward-facing step

Next, the measurement accuracy of the PTV system is discussed. The flow field to be measured is a turbulent flow field in a channel with a rearward-facing step as shown in **Fig. 12**. A 1.5-m long pipe of 0.1 × 0.1 m square section is installed upstream of the step, and a 2.0-m long pipe of 0.1 m × 0.15-m rectangular section is installed downstream of the step. The average velocity $U_0$ of the main flow upstream of the step is 0.8 m/s.

The flow field was visualized at the longitudinal section x-y at the center of the channel. The longitudinal section x-y was illuminated with the LLS from above the channel. The images were photographed with a camera in the direction normal to the longitudinal section x-y. The tracer particles used for the visualization were nylon particles with an average diameter of 50 $\mu$m and specific gravity of 1.02.

**Fig. 13**(a) shows the velocity vectors on the grid, and **Fig. 13**(b) shows the stream function calculated from the velocity information by the elliptic Poisson equation.

The reattachment points in this experiment are x/h-6.8. Next, these measurement results were compared with the results measured by laser Doppler velocimetry (LDV). **Fig. 14** shows the velocity distribution at x/h = 6.22. The solid circles indicate the PTV results, and the broken line indicates the LDV results. The vertical axis is made dimensionless by $U_0$. The two sets of results agree well with each other, although some differences are recognized in the shear layer and the recirculation region. This means that the PIV system can measure velocities with high reliability.

## 7. Velocity Measurement by PIV

PTV is a technique whereby velocity is measured from the tracer particle position at each time interval by an originally developed tracer tracking algorithm. The PTV technique is effective in measuring time-averaged velocity as already described. However, the PTV technique has several restrictions. One restriction is that it is difficult to apply PTV to the visualization of submicron tracer particles because velocity is measured from the position of tracer particles at specific times. Another is that it is necessary to uniformly add the tracer particles to the visualization space to measure instantaneous velocity. The authors have started work on the development of PIV as a technique for measuring the velocity of a fluid from the images of the fluid visualized with submicron tracer particles. The PIV technique is an image processing and measuring technique whereby the velocity of a fluid is measured from the similarity of the density distribution of the images photographed at a time interval. An algorithm has been already developed for measuring the velocity of a fluid from the density distribution of the visualization images photographed twice. This chapter describes velocity measurement by the PIV technique and the results of basic air flow experiments using the PIV technique.

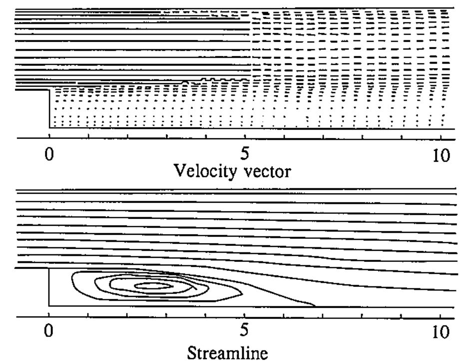


Fig. 13 Measurement of velocity around rearward-facing step

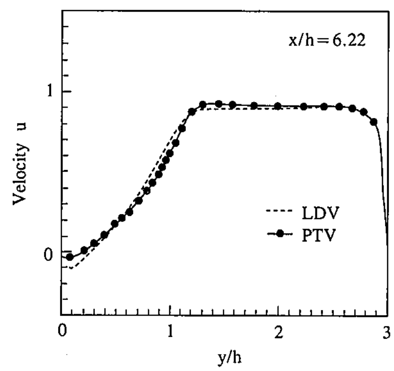


Fig. 14 PIV and LDV results

### 7.1 Preparation of processing images

In this image analysis, the velocity of fluid flow is measured from the images of the fluid photographed at two different times. First, images of submicron tracer particles are photographed with the visualization optical system shown in **Fig. 1** and input into the frame board of the image processing system shown in **Fig. 3**. When the tracer particles move over a long distance in the visualizing space, the light is directed onto the TV camera on a per-field basis as already described. The velocity of the fluid is measured from the tracer particle images photographed when illuminated with the LLS in the first and second fields. When the tracer particles move over a shorter distance, the light is directed onto the TV camera on a per-frame basis. The tracer particles are illuminated with the LLS once in the second field, and the tracer particles are tracked in the frame images obtained. When tracking the tracer particles in the field images, it is necessary to separate each frame input image into the first and second fields. This separation is made by Eq. (3), using the 3 × 3 mask of **Fig. 5**.

**7.2 Determination of velocity vectors**

The tracer particle images prepared by the above-mentioned procedure are processed as follows. The output of the TV camera is A/D converted on the frame memory of the image processing system into an image with 512 × 480 pixels, 8 bits, and 256 intensity levels in the horizontal and vertical directions. Input images are produced twice: the image produced at the time T1 is called F1, and the image produced at the time T2 is called F2. The PIV system performs cross-correlation calculation on the 8-bits, 256-intensity level images and takes the peak density positions as velocity vectors. The algorithm for measuring velocity from visualization images obtained with submicron tracer particles is explained below. First, a template region called MAsle of arbitrary size is established on the image photographed at the time T1. Next, a region of the same size as the template is moved on the image photographed at the time T2, and the density correlation is calculated by Eq. (5).

$$CR=\frac{\Sigma X_{ij}Y_{ij}-\frac{1}{n}\Sigma X_{ij}\Sigma Y_{ij}}{\sqrt{\Sigma X_{ij}{}^{2}-\frac{1}{n}(\Sigma X_{ij})^{2}}\sqrt{\Sigma Y_{ij}{}^{2}-\frac{1}{n}(\Sigma Y_{ij})^{2}}} \quad \cdots\cdots(5)$$

where $X_{ij}$ and $Y_{ij}$ are the image densities of pixels at the times T1 and T2. The obtained density correlation distribution is statistically processed to detect peak positions in the correlation distribution. Velocity vectors are determined from the center of the template region at the time T1 and the peak positions of the correlation distribution. This calculation is performed at an arbitrary position on the image taken at the time T1 to measure the velocity at an arbitrary position in the visualization space. If the template region is 50 × 50 and the velocity vectors to be measured are 31 × 31 points in the visualization space, for example, the calculation must be performed 6 × $10^{11}$ times using Eq. (5).

## 8. Application Example of PIV System

**8.1 Measurement of air flow**

The results of the experiment conducted to measure air flow by the PIV system are presented here. The experimental object was Karman's vortex flow occurring behind a cylinder. A 20-mm diameter cylinder was installed in a 2-m long pipe of 10 cm × 10 cm cross section, and the region around the cylinder was visualized with a TV camera. The Reynolds number based on the cylinder diameter and the main stream velocity was 260. **Fig. 15** shows a flow visualization image. Tobacco smoke particles of 0.3 $\mu$m in diameter were used as tracer particles for visualization. Since the tracer particles move relatively little in the image processing space for velocity measurement when using the density correlation method, two images were taken per frame using the electronic shutter of the TV camera, and instantaneous images were produced by the frame-to-field separation. A 41 × 41 template region was used to measure velocity from the two images photographed.

**Fig. 16** shows instantaneous velocity vectors measured by the PIV technique. A structural grid based on the harmony function theory was formed in the visualization space. Velocity was measured by the cross-correlation technique and spatially interpolated on a 31 × 31 equally-spaced grid by the method of Eq. (4).

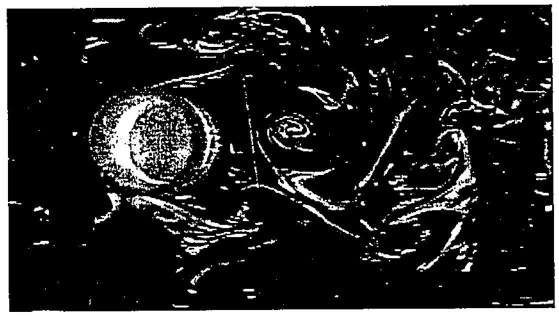

**Fig. 15** Visualization image of Karman's vortex behind cylinder

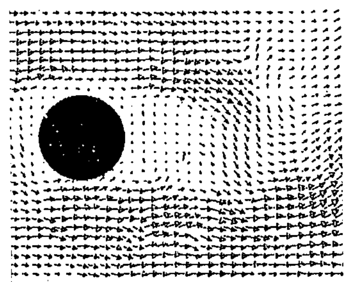

**Fig. 16** Velocity vectors on grid points

**8.2 Measurement of liquid velocity in two-phase flow of gas and liquid**[6]

Finally, an example of measuring the velocity of a liquid in a two-phase flow of gas and liquid by the PIV technique is described. As discussed above, the PTV and PIV techniques measure velocities from the positions of tracer particles at multiple times. When the PIV technique is applied to the measurement of liquid velocity in a two-phase flow of gas and liquid, an image processing method is required to distinguish between the tracer particles and the gas. The authors have already developed an algorithm for separating the tracer particles from the gas by using differences in circularity and scattered wave length. Even when this algorithm is used, it is still difficult to distinguish between fine gas bubbles and tracer particles. This section outlines flow visualization by the laser-induced fluorescence (LIF) method and describes the results of the laser-induced fluorescence method applied to the two-phase flow of gas and liquid.

The laser-induced fluorescence method adds a fluorescent material to a fluid and visualizes the flow field by imaging the laser-excited fluorescence of the fluorescent material. Zinc sulfide (ZnS), for example, absorbs 315-nm laser light and produces excited fluorescence. Its fluorescent light exhibits an afterglow of several seconds. This fluorescent light alone is imaged to separate the scattered light emitted by the gas from the excited light emitted by the liquid, and to measure the velocity of the liquid alone. The authors are studying the application of the afterglow of the fluorescent material to the measurement of the liquid velocity in the two-phase gas-liquid flow. An excited fluorescent image of a 1/25-scale model of a ladle is shown in **Fig. 17**, and processed

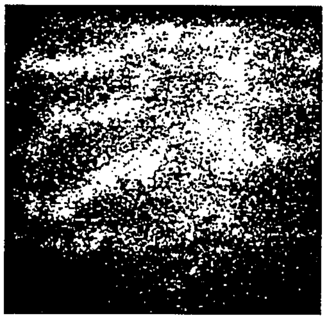

**Fig. 17** Excited fluorescent image by LIF

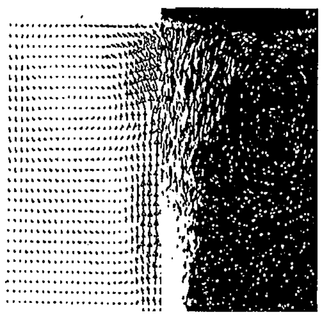

**Fig. 18** Measured liquid velocity vectors in two-phase flow of gas and liquid

liquid velocity vectors are shown in **Fig. 18**. In **Fig. 18**, the measured liquid velocity vectors are shown in the left side, and a gas bubble image visualized with a halogen lamp is shown in the right side. It is evident that the laser-induced fluorescence method can measure the velocity of the liquid in the flow field where the liquid is mixed with the gas.

## 9. Conclusions

A quantitative full-field velocity measurement system composed of a visualization system, an image processing system and image analysis software was developed and applied as an on-line velocimeter for a wide range of flow fields.

### References

1) Hesselink, L.: Annu. Rev. Fluid Mech. 20, 421-485 (1988)
2) Adrian, R.J.: Annu. Rev. Fluid Mech. 23, 261-304 (1991)
3) Khaligi, B., Huebler, M.S.: A Transient Water Analog of a Dual-Intake-Valve Engine for Intake Flow Visualization and Full-Field Vector Measurements, SAF Tech. Paper Series. 880519, 1988
4) Adamczyk, A.A., Rimal, L.: Reconstruction of 3-Dimensional Flow Field from Orthogonal View of Seed Track Video Images, Exp. Fluid. 6 1988, p. 380-386
5) Tsuda, N., Kobayashi, T., Saga, T.: Development of A Real-Time Velocity Measurement System for High Reynolds Fluid Flow Using Digital Image Processing Design, Experimental and Numerical Flow Visualization. ASME, 1992, p. 9-14
6) Tsuda, N., Kobayashi, T., Ohba, K., Saga, T. : Full Field Velocity Measurement in an Flow and a Two-Phase Flow by Using a Cross-Correlation Method, Proc. FLUCOM'94. Aug. 1994, p. 303-307